Journal of Applied Analysis and Computation
Volume 13, Number 5, October 2023, 2874–2895
Website:http://www.jaac-online.com
DOI:10.11948/20230044

# A NEW NUMERICAL APPROACH OF SOLVING FRACTIONAL MOBILE-IMMOBILE TRANSPORT EQUATION USING ATANGANA-BALEANU DERIVATIVE

Reetika Chawla[1,†], Komal Deswal[1] and Devendra Kumar[1]

**Abstract** A numerical scheme comprising the Crank-Nicolson difference scheme in the temporal direction and cubic trigonometric $B$-spline method in the spatial direction is examined for the numerical solution of the variable coefficient time-fractional mobile-immobile solute transport equation. The time-fractional derivative is evaluated using the Atangana-Baleanu Caputo derivative. The equation has advection, dispersion, and reaction coefficients that can be influenced simultaneously by space and time variables. The present numerical scheme is unconditionally stable and second-order convergent in the temporal and spatial directions. Several test problems are solved to confirm the theoretical results.

**Keywords** Atangana-Baleanu Caputo derivative, cubic trigonometric $B$-splines, Crank-Nicolson scheme, stability, convergence.

**MSC(2010)** 26A33, 65M06, 65M12, 65M15, 65N06, 65N15, 35R11.

## 1. Introduction

In recent times, fractional calculus is constantly evolving and has wide applications in various real-world phenomena [20, 28]. The integer order derivative being a local operator, may not be enough to explain physical phenomena, so the non-local operator in the form of a fractional-order derivative is used to study the physical and chemical processes accurately. Various applications in the fields of applied sciences [2], biology [27], and engineering [14, 31] have been discovered that can be investigated using fractional derivatives.

The most active area of research in fractional calculus is fractional differential equations that can represent complicated processes. Various numerical methods have been developed to solve these equations. Numerical methods such as finite volume method [22], meshless method [19], spectral method [34], discontinuous Galerkin method [23], compact finite difference scheme [9], finite element method [15,37] are used to solve and to evaluate the analytical solutions of various fractional partial differential equations.

†The corresponding author.
[1]Department of Mathematics, Birla Institute of Technology and Science, Pilani, Rajasthan-333031, India
Email: reetika.chawla285@gmail.com(R. Chawla), komaldeswal94@gmail.com(K. Deswal), dkumar@pilani.bits-pilani.ac.in(D. Kumar)

In a heterogeneous soil system, transport may allow for rapid movement of contaminants, with important implications for geochemical interaction and groundwater quality. There are two models that can efficiently describe the solute transport process; one of them was studied by Advection-Dispersion Equation (ADE) [5], and the other one is Mobile-Immobile Model (MIM) [8]. The MIM is distinct from ADE as it examines the solute exchange process between the flowing (mobile) and the stagnant (immobile) region in porous media, which is not explained by using ADE. The solute transport process was well explained by Li [21], and Gao [8] using MIM. The time-fractional MIM anticipates the continuous mass transfer to the immobile region from the mobile region. When the fractional-order $\alpha$ is less than unity, the solute continuously encounters the new immobile zones of the aquifer, and the continual transfer of mass can be examined by time-fractional MIM [31].

Fractional derivatives of several forms are discussed, including Grunwald-Leitnikov fractional derivatives, Riemann-Liouville fractional derivatives, Caputo fractional derivatives, etc. In 2015, Caputo and Fabrizio [4], a fractional derivative known as the Caputo-Fabrizio fractional derivative, was introduced. A nonsingular kernel is used in this fractional derivative to characterize the material heterogeneities and fluctuations on various scales better than those fractional derivatives that have a singular kernel [36]. After that, the generalized version of the Caputo-Fabrizio fractional derivative, known as the Atangana-Baleanu derivative, which has a non-local and nonsingular kernel, was introduced [1]. Recently, a few researchers have done numerical and analytical work using Atangana-Baleanu Caputo (ABC) derivative like in 2018, Bas and Ozarslan [2] presented some modeling problems that include population growth, Newton's law of cooling and blood alcohol using ABC derivative. Then in 2019, Gao *et al.* [10] discussed the viral diseases models for AIDS and Zika using this operator. Heydari and Atangana [16] discussed the optimization method based on Lucas polynomials to solve the space-time fractional mobile-immobile advection-dispersion equation. Later, in 2021, Shafiq *et al.* [33] used this fractional derivative and cubic B-spline functions to solve the time fractional advection-diffusion equation. Recently, Maayah *et al.* [26] presented the numerical solution of the cancer immune model using the ABC fractional derivative and the reproducing kernel scheme.

In 2018, a numerical approximation using tension spline was presented by Kanth for the time-fractional mobile-immobile advection-dispersion equation [17]. In 2020, Liu discovered the compact finite difference method for fractal mobile/immobile transport equation [25]. A numerical technique based on the operational matrix is presented for variable order time-fractional mobile-immobile equation by Ray [29] and Sadri [30]. Some more numerical methods such as spectral element method [32], orthogonal spline collocation method [35], finite difference method [24], finite element method [7], and meshless methods [11, 12] have been considered to examine this equation. According to the authors' best knowledge, none of them has considered the nonsingular ABC operator, which has a significant role in the models from fluid dynamics.

We consider the following time-fractional mobile-immobile solute transport equation [25] in the domain $\Omega \equiv \Omega_z \times \Omega_t = (0,1) \times (0,T]$:

$$ {}_0^{ABC}D_t^{\alpha} u + \beta(z,t)u_t - \nu(z,t)u_{zz} + \mu(z,t)u_z + \gamma(z,t)u = g(z,t), \quad (z,t) \in \Omega, \tag{1.1a} $$

with the initial condition

$$ u(z,0) = \psi(z), \text{ on } G_z = \overline{\Omega}_z \times \{0\}, \tag{1.1b} $$

and the boundary conditions

$$u(0,t) = \phi_0(t), \text{ on } G_0 = \{0\} \times \overline{\Omega}_t, \tag{1.1c}$$

$$u(1,t) = \phi_1(t), \text{ on } G_1 = \{1\} \times \overline{\Omega}_t, \tag{1.1d}$$

where $0 < \alpha < 1$ and $\partial\Omega = G_z \cup G_0 \cup G_1$ represents the boundary of the domain. The functions $\beta(z,t)$, $\nu(z,t)$, $\mu(z,t)$, and $\gamma(z,t)$, $\psi(z)$, $\phi_0(t)$, $\phi_1(t)$, and $g(z,t)$ are considered as sufficiently smooth functions. Furthermore, ${}_0^{ABC}D_t^{\alpha}u$ is the ABC time fractional derivative which is defined as [1, 33]

$${}_0^{ABC}D_t^{\alpha}u(z,t) = \frac{\mathfrak{N}_{\mathfrak{f}}(\alpha)}{1-\alpha}\int_0^t u'(z,s)E_{\alpha,1}\left[\frac{-\alpha}{1-\alpha}(t-s)^{\alpha}\right]ds,$$

where $\mathfrak{N}_{\mathfrak{f}}(\alpha)$ is termed as normalization function satisfying $\mathfrak{N}_{\mathfrak{f}}(0) = \mathfrak{N}_{\mathfrak{f}}(1) = 1$, and the term $E_{\alpha,\beta}(x)$ is defined as

$$E_{\alpha,\beta}(x) = \sum_{r=0}^{\infty}\frac{x^r}{\Gamma(\alpha r + \beta)}.$$

Several numerical methods with a low order of accuracy in the temporal direction are available for the solution of MIM [12, 17, 24, 25]. This work presents a numerical technique that involves the cubic trigonometric $B$-spline (CTBS) method in the spatial direction and the Crank-Nicolson difference scheme in the temporal direction to solve the problem (1.1). The advantage of applying the Crank-Nicolson implicit scheme using the ABC fractional operator is that it increases the order of accuracy in the temporal direction. As in [17, 25], the authors presented the numerical schemes that give $(2-\alpha)$ convergence order in the time direction. Trigonometric B-splines are a group of distinct spline functions that construct piecewise polynomials by identifying the correct linear combination. The computational benefit of these functions comes from the fact that each trigonometric spline basis function of order m is nonzero for a maximum of m consecutive intervals and zero otherwise. Due to their smoothness and ability to regulate local events, these basis functions are preferable to others. We investigate the fractional-order time derivative using a reliable numerical technique using the ABC derivative. As per our knowledge, the Crank-Nicolson-based ABC operator is explored here for the first time for this problem. Recently, this was discussed for a non-linear problem named time fractional BBMB equation [6]. The purpose of using this fractional operator in the form of the Crank-Nicolson scheme is that this problem has given low order of accuracy for $0 < \alpha < 1$ using the other operators. Our presented scheme gives high order of accuracy for the considered problem than the other implicit numerical schemes discussed in the literature. Through Fourier analysis, the scheme is demonstrated to be unconditionally stable. Furthermore, the present numerical scheme is shown as second-order convergent in spatial and temporal directions. The proposed numerical scheme is tested for two test examples to verify the theoretical results. Several surfaces and line plots are drawn to show the solution behavior.

The structure of this article is as follows. Section 2 presents the numerical technique that uses the ABC derivative to deal with the fractional time derivative. Section 3 proposes the Crank-Nicolson difference scheme using the CTBS method. Then, we analyze the unconditional stability using the Fourier analysis method in

Section 4, and the convergence of the presented numerical scheme is investigated in Section 5. At last, in Section 6, we introduced the numerical results that illustrate the integrity of the numerical method, followed by the conclusions in Section 7.

## 2. ABC derivative approximation

In this section, we introduce the equidistant mesh $\{t_q = q\tau,\ \tau = T/M_t,\ 0 \le q \le M_t\}$ in the temporal direction. We approximate the time-fractional derivative evaluated at $t_{q-1/2}$. Initially, we estimate the time-fractional derivative at $t_q$ and $t_{q-1}$, respectively, and then take the average to employ the Crank-Nicolson scheme.

Now, $f'(t)$ can be written as [33],

$$f'(t) = \frac{f(t_{q+1}) - f(t_q)}{\tau} - \frac{\tau}{2} f''(t_q) + O(\tau^2), \quad t \in (t_q, t_{q+1}). \tag{2.1}$$

At $t_q$ time level, the fractional derivative is approximated as follows

$$\begin{aligned}
{}_0^{ABC}D_t^{\alpha} f(t)|_{t=t_q} &= \frac{\mathfrak{N}_{\mathfrak{f}}(\alpha)}{1-\alpha} \int_0^{t_q} f'(s) E_{\alpha}\left[\frac{-\alpha}{1-\alpha}(t_q - s)^{\alpha}\right] ds \\
&= \frac{\mathfrak{N}_{\mathfrak{f}}(\alpha)}{1-\alpha} \sum_{j=0}^{q-1} \int_{t_j}^{t_{j+1}} f'(s) E_{\alpha}\left[\frac{-\alpha}{1-\alpha}(t_q - s)^{\alpha}\right] ds \\
&= \frac{\mathfrak{N}_{\mathfrak{f}}(\alpha)}{1-\alpha} \sum_{j=0}^{q-1} \int_{t_j}^{t_{j+1}} \frac{f(t_{j+1}) - f(t_j)}{\tau} E_{\alpha}\left[\frac{-\alpha}{1-\alpha}(t_q - s)^{\alpha}\right] ds + \mathfrak{R}_q \\
&= \frac{\mathfrak{N}_{\mathfrak{f}}(\alpha)}{1-\alpha} \sum_{j=0}^{q-1} \frac{f(t_{j+1}) - f(t_j)}{\tau} \Bigg\{ (t_q - t_j) E_{\alpha,2}\left[\frac{-\alpha}{1-\alpha}(t_q - t_j)^{\alpha}\right] \\
&\quad - (t_q - t_{j+1}) E_{\alpha,2}\left[\frac{-\alpha}{1-\alpha}(t_q - t_{j+1})^{\alpha}\right] \Bigg\} + \mathfrak{R}_q \\
&= \frac{\mathfrak{N}_{\mathfrak{f}}(\alpha)}{1-\alpha} \sum_{j=0}^{q} B_j^q f(t_j) + \mathfrak{R}_q.
\end{aligned}$$

The coefficients $B_j^q$ are expressed in terms of $E_j^q$ which is used to represent $E_{\alpha,2}\left[\frac{-\alpha}{1-\alpha}(t_q - t_j)^{\alpha}\right]$. The coefficients $B_j^q,\ q = 1, 2, \ldots, M_t$ are defined as

$$B_j^q = \begin{cases} (q-1)E_1^q - qE_0^q, & j = 0, \\ (q-j+1)E_{j-1}^q - 2(q-j)E_j^q + (q-j-1)E_{j+1}^q, & 0 < j < q, \\ E_{q-1}^q, & j = q, \end{cases}$$

and $\mathfrak{R}_q$ is the truncation error calculated as

$$\begin{aligned}
\mathfrak{R}_q &= \frac{\mathfrak{N}_{\mathfrak{f}}(\alpha)}{1-\alpha} \sum_{j=0}^{q-1} \int_{t_j}^{t_{j+1}} \frac{\tau}{2} f''(t_j) E_{\alpha}\left[\frac{-\alpha}{1-\alpha}(t_q - s)^{\alpha}\right] ds \\
&= \frac{\mathfrak{N}_{\mathfrak{f}}(\alpha)}{1-\alpha} \frac{\tau^2}{2} \sum_{j=0}^{q-1} f''(t_j)[(q-j)E_j^q - (q-j-1)E_{j+1}^q].
\end{aligned}$$

Thus,

$$|\Re_q| \le C_1 \frac{\mathfrak{N}_{\mathfrak{f}}(\alpha)}{1-\alpha}\frac{\tau^2}{2}\left[\max_{0\le t\le t_{q-1}}|f''(t)|\right],$$

where $C_1$ is a constant.

Now, the evaluation of ABC derivative at $t = t_{q-1}$ time level is given as

$$\begin{aligned}
&{}_0^{ABC}D_t^{\alpha} f(t)|_{t=t_{q-1}} \\
&= \frac{\mathfrak{N}_{\mathfrak{f}}(\alpha)}{1-\alpha}\int_0^{t_{q-1}} f'(s)E_{\alpha}\left[\frac{-\alpha}{1-\alpha}(t_{q-1}-s)^{\alpha}\right]ds \\
&= \frac{\mathfrak{N}_{\mathfrak{f}}(\alpha)}{1-\alpha}\sum_{j=0}^{q-2}\int_{t_j}^{t_{j+1}} f'(s)E_{\alpha}\left[\frac{-\alpha}{1-\alpha}(t_{q-1}-s)^{\alpha}\right]ds \\
&= \frac{\mathfrak{N}_{\mathfrak{f}}(\alpha)}{1-\alpha}\sum_{j=0}^{q-2}\int_{t_j}^{t_{j+1}} \frac{f(t_{j+1})-f(t_j)}{\tau}E_{\alpha}\left[\frac{-\alpha}{1-\alpha}(t_{q-1}-s)^{\alpha}\right]ds + \Re_{q-1} \\
&= \frac{\mathfrak{N}_{\mathfrak{f}}(\alpha)}{1-\alpha}\sum_{j=0}^{q-2}\frac{f(t_{j+1})-f(t_j)}{\tau}\left\{(t_{q-1}-t_j)E_{\alpha,2}\left[\frac{-\alpha}{1-\alpha}(t_{q-1}-t_j)^{\alpha}\right]\right. \\
&\left. - (t_{q-1}-t_{j+1})E_{\alpha,2}\left[\frac{-\alpha}{1-\alpha}(t_{q-1}-t_{j+1})^{\alpha}\right]\right\} + \Re_{q-1} \\
&= \frac{\mathfrak{N}_{\mathfrak{f}}(\alpha)}{1-\alpha}\sum_{j=0}^{q-1} D_j^{q-1} f(t_j) + \Re_{q-1},
\end{aligned}$$

where the coefficients $D_j^{q-1}$, $q = 2, 3, \ldots, M_t$ are defined as

$$D_j^{q-1} = \begin{cases} (q-2)E_1^{q-1} - (q-1)E_0^{q-1}, & j = 0, \\ (q-j)E_{j-1}^{q-1} - 2(q-j-1)E_j^{q-1} + (q-j-2)E_{j+1}^{q-1}, & 0 < j < q-1, \\ E_{q-2}^{q-1}, & j = q-1, \end{cases}$$

and $D_0^0 = 0$. The error term $\Re_{q-1}$ is calculated as follows

$$\begin{aligned}
\Re_{q-1} &= \frac{\mathfrak{N}_{\mathfrak{f}}(\alpha)}{1-\alpha}\sum_{j=0}^{q-2}\int_{t_j}^{t_{j+1}} \frac{\tau}{2}f''(t_j)E_{\alpha}\left[\frac{-\alpha}{1-\alpha}(t_{q-1}-s)^{\alpha}\right]ds \\
&= \frac{\mathfrak{N}_{\mathfrak{f}}(\alpha)}{1-\alpha}\frac{\tau^2}{2}\sum_{j=0}^{q-1} f''(t_j)[(q-j-1)E_j^{q-1} - (q-j-2)E_{j+1}^{q-1}].
\end{aligned}$$

So,

$$|\Re_{q-1}| \le C_2 \frac{\mathfrak{N}_{\mathfrak{f}}(\alpha)}{1-\alpha}\frac{\tau^2}{2}\left[\max_{0\le t\le t_{q-2}}|f''(t)|\right],$$

where $C_2$ is a constant.

Now, at $t = t_{q-1/2}$ time level, we have

$${}_0^{ABC}D_t^{\alpha} f(t)|_{t=t_{q-1/2}} = \frac{{}_0^{ABC}D_t^{\alpha} f(t)|_{t=t_q} + {}_0^{ABC}D_t^{\alpha} f(t)|_{t=t_{q-1}}}{2}$$

$$= \frac{\mathfrak{N}_{\mathfrak{f}}(\alpha)}{2(1-\alpha)}\left[\sum_{j=0}^{q} B_j^q f(t_j) + \sum_{j=0}^{q-1} D_j^{q-1} f(t_j)\right] + \mathfrak{R}_{q-1/2}, \quad (2.2)$$

where $\mathfrak{R}_{q-1/2}$ at $t = t_{q-1/2}$ satisfies

$$|\mathfrak{R}_{q-1/2}| \leq \frac{|\mathfrak{R}_q| + |\mathfrak{R}_{q-1}|}{2} \leq C\frac{\mathfrak{N}_{\mathfrak{f}}(\alpha)}{1-\alpha}\frac{\tau^2}{2}\left[\max_{0\leq t\leq t_{q-1}} |f''(t)| + \max_{0\leq t\leq t_{q-2}} |f''(t)|\right], \quad (2.3)$$

where $C = \max\{C_1, C_2\}$.

From equation (2.2) and (2.3), we obtain

$${}_0^{ABC}D_t^{\alpha} f(t)|_{t=t_{q-1/2}} = S\left(\sum_{j=0}^{q} B_j^q f(t_j) + \sum_{j=0}^{q-1} D_j^{q-1} f(t_j)\right) + O(\tau^2), \quad (2.4)$$

where $S = \frac{\mathfrak{N}_{\mathfrak{f}}(\alpha)}{2(1-\alpha)}$.

# 3. The Crank-Nicolson CTBS numerical scheme

In this section, we will obtain the Crank-Nicolson difference scheme using the CTBS method for evaluating the numerical solution of the time-fractional mobile-immobile solute transport equation (1.1). The domain $0 \leq z \leq 1$ is equally partitioned into $N_z$ subintervals by nodes $z_n, n = 0, 1, \ldots, N_z$ of equal length $h = \frac{1}{N_z}$. We are using CTBS to seek an approximate solution $U(z,t)$ of the equation (1.1) in the following form

$$U(z,t) = \sum_{n=-1}^{N_z-1} \varrho_n(t) TB_n(z), \quad (3.1)$$

where $\varrho_n(t)$ are time-dependent unknowns that have to be determined, and $TB_n$ are the twice differentiable cubic trigonometric basis functions that are given as

$$TB_n(z) = \frac{1}{w}\begin{cases} p^3(z_n), & z \in [z_n, z_{n+1}], \\ p(z_n)(p(z_n)r(z_{n+2}) + r(z_{n+3})p(z_{n+1})) & \\ +r(z_{n+4})p^2(z_{n+1}), & z \in [z_{n+1}, z_{n+2}], \\ r(z_{n+4})(p(z_{n+1})r(z_{n+3}) + r(z_{n+4})p(z_{n+2})) & \\ +p(z_n)r^2(z_{n+3}), & z \in [z_{n+2}, z_{n+3}], \\ r^3(z_{n+4}), & z \in [z_{n+3}, z_{n+4}], \end{cases} \quad (3.2)$$

where $p(z_n) = \sin\left(\frac{z-z_n}{2}\right)$, $r(z_n) = \sin\left(\frac{z_n-z}{2}\right)$, $w = \sin\left(\frac{h}{2}\right)\sin(h)\sin\left(\frac{3h}{2}\right)$.

The conditions (1.1b), (1.1c) and (1.1d) as well as the collocation conditions on $TB_n(z)$, are used to obtain an approximation for $U_n^q$ and its derivatives given by

$$\begin{cases} U_n^q = a_1\varrho_{n-1}^q + a_2\varrho_n^q + a_1\varrho_{n+1}^q, \\ (U_z)_n^q = -a_3\varrho_{n-1}^q + a_3\varrho_{n+1}^q, \\ (U_{zz})_n^q = a_4\varrho_{n-1}^q + a_5\varrho_n^q + a_4\varrho_{n+1}^q, \end{cases} \quad (3.3)$$

where

$$a_1 = \csc(h)\csc\left(\frac{3h}{2}\right)\sin^2\left(\frac{3h}{2}\right), \quad a_2 = \frac{2}{1+2\cos(h)}, \quad a_3 = \frac{3}{4}\csc\left(\frac{3h}{2}\right),$$
$$a_4 = \frac{3+9\cos(h)}{4\cos(\frac{h}{2})-4\cos(\frac{5h}{2})}, \quad a_5 = -\frac{3\cot^2(\frac{h}{2})}{2+4\cos(h)}.$$

Using (2.2) and on applying the Crank-Nicolson scheme at the $(q-1/2)$-th level, the equation (1.1) can be written as

$$S\left(\sum_{j=0}^{q} B_j^q + \sum_{j=0}^{q-1} D_j^{q-1}\right)u_n^j + \beta_n^{q-1/2}\left(\frac{u_n^q - u_n^{q-1}}{\tau}\right) - \nu_n^{q-1/2}\left(\frac{(u_{zz})_n^q + (u_{zz})_n^{q-1}}{2}\right)$$
$$+ \mu_n^{q-1/2}\left(\frac{(u_z)_n^q + (u_z)_n^{q-1}}{2}\right) + \gamma_n^{q-1/2}\left(\frac{u_n^q + u_n^{q-1}}{2}\right) = g(z_n, t_{q-1/2}),\ q = 1, 2, \ldots, M_t. \tag{3.4}$$

After plugging in the approximations $U_n^q$ and their derivatives from (3.3) into equation (3.4), we obtain the following fully discretized numerical scheme at the $(q-\frac{1}{2})$-th level

$$\left(SB_q^q + \frac{\hat{\beta}}{\tau} + \frac{\hat{\gamma}}{2}\right)[a_1\varrho_{n-1}^q + a_2\varrho_n^q + a_1\varrho_{n+1}^q] - \frac{\hat{\nu}}{2}[a_4\varrho_{n-1}^q + a_5\varrho_n^q + a_4\varrho_{n+1}^q]$$
$$+ \frac{\hat{\mu}}{2}[-a_3\varrho_{n-1}^q + a_3\varrho_{n+1}^q]$$
$$= \left(-SD_{q-1}^{q-1} + \frac{\hat{\beta}}{\tau} - \frac{\hat{\gamma}}{2}\right)[a_1\varrho_{n-1}^{q-1} + a_2\varrho_n^{q-1} + a_1\varrho_{n+1}^{q-1}] + \frac{\hat{\nu}}{2}[a_4\varrho_{n-1}^{q-1} + a_5\varrho_n^{q-1} + a_4\varrho_{n+1}^{q-1}]$$
$$- \frac{\hat{\mu}}{2}[-a_3\varrho_{n-1}^{q-1} + a_3\varrho_{n+1}^{q-1}] - S\left(\sum_{j=0}^{q-1} B_j^q + \sum_{j=0}^{q-2} D_j^{q-1}\right)[a_1\varrho_{n-1}^j + a_2\varrho_n^j + a_1\varrho_{n+1}^j]$$
$$+ g(z_n, t_{q-1/2}),\ q = 1, 2, \ldots, M_t. \tag{3.5}$$

**Remark 3.1.** For simplicity, the variable coefficients considered at the $(q-1/2)$-th level *i.e.,* $\beta_n^{q-1/2}$, $\nu_n^{q-1/2}$, $\mu_n^{q-1/2}$, and $\gamma_n^{q-1/2}$ are represented as $\hat{\beta}$, $\hat{\nu}$, $\hat{\mu}$, and $\hat{\gamma}$, respectively.

The equation (3.5) can further be written as

$$\left[\left(SB_q^q + \frac{\hat{\beta}}{\tau} + \frac{\hat{\gamma}}{2}\right)a_1 - \frac{\hat{\nu}}{2}a_4 - \frac{\hat{\mu}}{2}a_3\right]\varrho_{n-1}^q + \left[\left(SB_q^q + \frac{\hat{\beta}}{\tau} + \frac{\hat{\gamma}}{2}\right)a_2 - \frac{\hat{\nu}}{2}a_5\right]\varrho_n^q$$
$$+ \left[\left(SB_q^q + \frac{\hat{\beta}}{\tau} + \frac{\hat{\gamma}}{2}\right)a_1 - \frac{\hat{\nu}}{2}a_4 + \frac{\hat{\mu}}{2}a_3\right]\varrho_{n+1}^q$$
$$= \left[\left(-SD_{q-1}^{q-1} + \frac{\hat{\beta}}{\tau} - \frac{\hat{\gamma}}{2}\right)a_1 + \frac{\hat{\nu}}{2}a_4 + \frac{\hat{\mu}}{2}a_3\right]\varrho_{n-1}^{q-1} + \left[\left(-SD_{q-1}^{q-1} + \frac{\hat{\beta}}{\tau} - \frac{\hat{\gamma}}{2}\right)a_2 + \frac{\hat{\nu}}{2}a_5\right]\varrho_n^{q-1}$$
$$+ \left[\left(-SD_{q-1}^{q-1} + \frac{\hat{\beta}}{\tau} - \frac{\hat{\gamma}}{2}\right)a_1 + \frac{\hat{\nu}}{2}a_4 - \frac{\hat{\mu}}{2}a_3\right]\varrho_{n+1}^{q-1} - S\sum_{j=0}^{q-1} B_j^q[a_1\varrho_{n-1}^j + a_2\varrho_n^j + a_1\varrho_{n+1}^j]$$

$$- S\sum_{j=0}^{q-2} D_j^{q-1}[a_1\varrho_{n-1}^j + a_2\varrho_n^j + a_1\varrho_{n+1}^j] + g(z_n, t_{q-1/2}),\ q = 1, 2, \ldots, M_t. \quad (3.6)$$

The system presented by equation (3.6) comprises of $(N_z + 1)$ linear equations in $(N_z + 3)$ unknowns. The boundary conditions (1.1c) and (1.1d) are used to get two additional equations, and thus a unique solution to the system of dimension $(N_z + 3) \times (N_z + 3)$ is obtained.

### 3.1. Initial Vector $\boldsymbol{\varrho^0}$

It is essential to find the initial solution vector $\varrho^0 = [\varrho_{-1}^0, \varrho_0^0, \ldots, \varrho_{N_z+1}^0]$ to begin the iteration process. By using the initial condition and its derivatives at the two boundaries, we can evaluate the initial vector, which is given as follows

1. $(u_n^0)_z = \frac{d}{dz}\psi(z_n),\ n = 0,$
2. $u_n^0 = \psi(z_n),\ n = 1, 2, \ldots, N_z,$
3. $(u_n^0)_z = \frac{d}{dz}\psi(z_n),\ n = N_z.$

It forms a tri-diagonal system comprising of $(N_z + 3)$ linear equations in $(N_z + 3)$ unknowns which can be written in matrix form as

$$A\varrho^0 = b,$$

where

$$A = \begin{bmatrix} -a_3 & 0 & a_3 & \ldots & \ldots & \ldots & 0 \\ a_1 & a_2 & a_1 & & & & \vdots \\ 0 & a_1 & a_2 & a_1 & & & \vdots \\ \vdots & \ddots & \ddots & \ddots & & & \vdots \\ \vdots & & a_1 & a_2 & a_1 & & \vdots \\ \vdots & & & \ddots & \ddots & \ddots & \vdots \\ \vdots & & & & a_1 & a_2 & a_1 \\ 0 & \ldots & \ldots & \ldots & -a_3 & 0 & a_3 \end{bmatrix}$$

and $b = (\psi'(z_0), \psi(z_0), \ldots, \psi(z_{N_z}), \psi'(z_{N_z}))^T$.

## 4. Stability Analysis

We will use the Fourier analysis to explore the stability of the numerical scheme (3.6). First, we consider the error term $\xi_n^q = \varrho_n^q - \widetilde{\varrho}_n^q, 0 \le n \le N_z, 0 \le q \le M_t$ where $\varrho_n^q$ and $\widetilde{\varrho}_n^q$ is the growth factor and its approximation in Fourier mode. The error equation for $q = 1$ is given as

$$b_1\xi_{n-1}^1 + c_1\xi_n^1 + d_1\xi_{n+1}^1 = k_0\xi_{n-1}^0 + l_0\xi_n^0 + m_0\xi_{n+1}^0 - SB_0^1[a_1\xi_{n-1}^0 + a_2\xi_n^0 + a_1\xi_{n+1}^0], \quad (4.1)$$

while for $q > 1$, it is

$$\begin{aligned} & b_q\xi_{n-1}^q + c_q\xi_n^q + d_q\xi_{n+1}^q \\ =& k_{q-1}\xi_{n-1}^{q-1} + l_{q-1}\xi_n^{q-1} + m_{q-1}\xi_{n+1}^{q-1} - S\sum_{j=0}^{q-1} B_j^q[a_1\xi_{n-1}^j + a_2\xi_n^j + a_1\xi_{n+1}^j] \\ & - S\sum_{j=0}^{q-2} D_j^{q-1}[a_1\xi_{n-1}^j + a_2\xi_n^j + a_1\xi_{n+1}^j], \end{aligned} \tag{4.2}$$

where the coefficients are given as

$$\begin{aligned} & b_q = \left(SB_q^q + \frac{\hat{\beta}}{\tau} + \frac{\hat{\gamma}}{2}\right)a_1 - \frac{\hat{\nu}}{2}a_4 - \frac{\hat{\mu}}{2}a_3,\ c_q = \left(SB_q^q + \frac{\hat{\beta}}{\tau} + \frac{\hat{\gamma}}{2}\right)a_2 - \frac{\hat{\nu}}{2}a_5, \\ & d_q = \left(SB_q^q + \frac{\hat{\beta}}{\tau} + \frac{\hat{\gamma}}{2}\right)a_1 - \frac{\hat{\nu}}{2}a_4 + \frac{\hat{\mu}}{2}a_3,\ k_{q-1} = \left(-SD_{q-1}^{q-1} + \frac{\hat{\beta}}{\tau} - \frac{\hat{\gamma}}{2}\right)a_1 + \frac{\hat{\nu}}{2}a_4 + \frac{\hat{\mu}}{2}a_3, \\ & l_{q-1} = \left(-SD_{q-1}^{q-1} + \frac{\hat{\beta}}{\tau} - \frac{\hat{\gamma}}{2}\right)a_2 + \frac{\hat{\nu}}{2}a_5,\ m_{q-1} = \left(-SD_{q-1}^{q-1} + \frac{\hat{\beta}}{\tau} - \frac{\hat{\gamma}}{2}\right)a_1 + \frac{\hat{\nu}}{2}a_4 - \frac{\hat{\mu}}{2}a_3, \end{aligned}$$

where $q = 1, 2, \ldots, M_t$.

The grid function is defined as [24],

$$\xi^q(z) = \begin{cases} 0, & 0 \le z \le z_{\frac{1}{2}}, \\ \xi_n^q, & z_{n-\frac{1}{2}} \le z \le z_{n+\frac{1}{2}}, \quad 1 \le n \le N_z - 1, \\ 0, & z_{N_z-\frac{1}{2}} \le z \le z_{N_z}. \end{cases}$$

The Fourier series expansion of $\xi^q(z)$ is

$$\xi^q(z) = \sum_{j=-\infty}^{\infty} \rho_q(j) e^{\frac{i2\pi jz}{L}}, \quad q = 0, 1, \ldots, M_t,$$

where

$$\rho_q(j) = \frac{1}{L}\int_0^L \xi^q(\zeta) e^{\frac{-i2\pi j\zeta}{L}} d\zeta,$$

are called the Fourier coefficients.

We initiate Parseval's identity

$$\int_0^L |\xi^q(z)|^2 dz = \sum_{j=-\infty}^{\infty} |\rho_q(j)|^2,$$

and the norm

$$\|\xi^q\|_2 = \left(\sum_{n=1}^{N_z-1} h|\xi_n^q|^2\right)^{\frac{1}{2}} = \left(\int_0^L |\xi^q(z)|^2 dz\right)^{\frac{1}{2}},$$

we have

$$\|\xi^q\|_2^2 = \sum_{j=-\infty}^{\infty} |\rho_q(j)|^2. \tag{4.3}$$

Consider the form $\xi_n^q = \rho_q e^{i\omega nh}$, where $\omega = 2\pi j/L$ and $L = 1$ to represent the solution of (4.1) and (4.2). Thus, for $q = 1$, we obtain

$$(b_1e^{-i\omega h}+c_1+d_1e^{i\omega h})\rho_1=[k_0e^{-i\omega h}+l_0+m_0e^{i\omega h}-SB_0^1(a_1e^{-i\omega h}+a_2+a_1e^{i\omega h})]\rho_0, \tag{4.4}$$

and for $q > 1$, it gives

$$\begin{aligned}&(b_qe^{-i\omega h} + c_q + d_qe^{i\omega h})\rho_q\\ =&(k_{q-1}e^{-i\omega h} + l_{q-1} + m_{q-1}e^{i\omega h})\rho_{q-1} - S\sum_{j=0}^{q-1} B_j^q(a_1e^{-i\omega h} + a_2 + a_1e^{i\omega h})\rho_j\\ &- S\sum_{j=0}^{q-2} D_j^{q-1}(a_1e^{-i\omega h} + a_2 + a_1e^{i\omega h})\rho_j.\end{aligned} \tag{4.5}$$

After simplifying, the equation (4.4) gives

$$\begin{aligned}|\rho_1| &= \left|\frac{(k_0 + m_0)\cos\omega h + i(-k_0 + m_0)\sin\omega h + l_0 - SB_0^1(2a_1\cos\omega h + a_2)}{(b_1 + d_1)\cos\omega h + i(-b_1 + d_1)\sin\omega h + c_1}\right||\rho_0|\\ &= \left|\frac{\left(\frac{\hat\beta}{\tau} - S(D_0^0+B_0^1) - \frac{\hat\gamma}{2}\right)(2a_1\cos\omega h+a_2)+\frac{\hat\nu}{2}(2a_4\cos\omega h+a_5)+i(-\hat\mu a_3)\sin\omega h}{\left(\frac{\hat\beta}{\tau}+SB_1^1+\frac{\hat\gamma}{2}\right)(2a_1\cos\omega h+a_2)-\frac{\hat\nu}{2}(2a_4\cos\omega h+a_5)+i(\hat\mu a_3)\sin\omega h}\right||\rho_0|\\ &= \sqrt{\frac{\left(1 - \frac{SB_0^1\tau}{\hat\beta} - \frac{\hat\gamma\tau}{2\hat\beta} + \frac{\hat\nu\tau}{2\hat\beta}\kappa\right)^2 + \left((-\hat\mu a_3)\vartheta\tau\sin\omega h\right)^2}{\left(1 + \frac{SB_1^1\tau}{\hat\beta} + \frac{\hat\gamma\tau}{2\hat\beta} - \frac{\hat\nu\tau}{2\hat\beta}\kappa\right)^2 + \left((\hat\mu a_3)\vartheta\tau\sin\omega h\right)^2}}|\rho_0|,\end{aligned} \tag{4.6}$$

where $\kappa = \dfrac{2a_4\cos\omega h + a_5}{2a_1\cos\omega h + a_2}$ and $\vartheta = \dfrac{1}{\hat\beta(2a_1\cos\omega h + a_2)}$. As $\tau \to 0$, we obtain $|\rho_1| \le |\rho_0|$.

Let the condition $|\rho_s| \le |\rho_0|$ holds true $\forall\ s = 2, 3, \ldots, q-1$. Then, we will prove that the condition holds for $s = q$. From Equation (4.5), we have

$$\begin{aligned}|\rho_q| =&\left|\frac{[(k_{q-1} + m_{q-1})\cos\omega h + i(-k_{q-1} + m_{q-1})\sin\omega h + l_{q-1}]\rho_{q-1}}{(b_q + d_q)\cos\omega h + i(-b_q + d_q)\sin\omega h + c_q}\right|\\ &+\left|\frac{-S(\sum_{j=0}^{q-1} B_j^q + \sum_{j=0}^{q-2} D_j^{q-1})(2a_1\cos\omega h + a_2)\rho_j}{(b_q + d_q)\cos\omega h + i(-b_q + d_q)\sin\omega h + c_q}\right|\\ \le&\frac{|(k_{q-1} + m_{q-1})\cos\omega h + i(-k_{q-1} + m_{q-1})\sin\omega h + l_{q-1}|}{|(b_q + d_q)\cos\omega h + i(-b_q + d_q)\sin\omega h + c_q|}|\rho_0|\\ &+\frac{(2a_1\cos\omega h + a_2)| - S(\sum_{j=0}^{q-1} B_j^q + \sum_{j=0}^{q-2} D_j^{q-1})||\rho_j|}{|(b_q + d_q)\cos\omega h + i(-b_q + d_q)\sin\omega h + c_q|}.\end{aligned}$$

Using the conditions $\sum_{j=0}^{q} B_j^q = 0$ and $\sum_{j=0}^{q-1} D_j^{q-1} = 0$, we get

$$
\begin{aligned}
|\rho_q| \leq & \left| \frac{\left(\frac{\hat{\beta}}{\tau} - SD_{q-1}^{q-1} - \frac{\hat{\gamma}}{2}\right)(2a_1\cos\omega h + a_2) + \frac{\hat{\nu}}{2}(2a_4\cos\omega h + a_5) + i(-\hat{\mu}a_3)\sin\omega h}{\left(\frac{\hat{\beta}}{\tau} + SB_q^q + \frac{\hat{\gamma}}{2}\right)(2a_1\cos\omega h + a_2) - \frac{\hat{\nu}}{2}(2a_4\cos\omega h + a_5) + i(\hat{\mu}a_3)\sin\omega h} \right| |\rho_0| \\
& + \frac{(2a_1\cos\omega h + a_2)(SB_q^q + SD_{q-1}^{q-1})}{\left| \left(\frac{\hat{\beta}}{\tau} + SB_q^q + \frac{\hat{\gamma}}{2}\right)(2a_1\cos\omega h + a_2) - \frac{\hat{\nu}}{2}(2a_4\cos\omega h + a_5) + i(\hat{\mu}a_3)\sin\omega h \right|} |\rho_0| \\
= & \sqrt{\frac{\left(1 - \frac{SD_{q-1}^{q-1}\tau}{\hat{\beta}} - \frac{\hat{\gamma}\tau}{2\hat{\beta}} + \frac{\hat{\nu}\tau}{2\hat{\beta}}\kappa\right)^2 + \left((-\hat{\mu}a_3)\vartheta\tau\sin\omega h\right)^2}{\left(1 + \frac{SB_q^q\tau}{\hat{\beta}} + \frac{\hat{\gamma}\tau}{2\hat{\beta}} - \frac{\hat{\nu}\tau}{2\hat{\beta}}\kappa\right)^2 + \left((\hat{\mu}a_3)\vartheta\tau\sin\omega h\right)^2}} |\rho_0| \\
& + \frac{\tau(SB_q^q + SD_{q-1}^{q-1})}{\hat{\beta}\sqrt{\left(1 + \frac{SB_q^q\tau}{\hat{\beta}} + \frac{\hat{\gamma}\tau}{2\hat{\beta}} - \frac{\hat{\nu}\tau}{2\hat{\beta}}\kappa\right)^2 + \left((\hat{\mu}a_3)\vartheta\tau\sin\omega h\right)^2}} |\rho_0|.
\end{aligned}
$$

As $\tau \to 0$, we acquire the following condition

$$|\rho_q| \leq |\rho_0|. \tag{4.7}$$

Using the equation (4.3) along with (4.7) we obtain

$$\|\xi^q\|_2 \leq \|\xi^0\|_2, \quad \forall\ q = 0, 1, \ldots, M_t. \tag{4.8}$$

Hence, the present numerical scheme is unconditionally stable.

## 5. Convergence Analysis

We require some results presented in this section to deal with the convergence.

To begin the convergence analysis, we rewrite the scheme (3.4) as

$$
\begin{aligned}
& S\tau\left(\sum_{j=0}^{q} B_j^q + \sum_{j=0}^{q-1} D_j^{q-1}\right)u_n^j + \hat{\beta}(u_n^q - u_n^{q-1}) - \hat{\nu}\tau\left(\frac{(u_{zz})_n^q + (u_{zz})_n^{q-1}}{2}\right) \\
& + \hat{\mu}\tau\left(\frac{(u_z)_n^q + (u_z)_n^{q-1}}{2}\right) + \hat{\gamma}\tau\left(\frac{u_n^q + u_n^{q-1}}{2}\right) \\
= & \tau g(z_n, t_{q-1/2}), \quad q = 1, 2, \ldots, M_t.
\end{aligned} \tag{5.1}
$$

Now in equation (5.1), the CTBS is applied by substituting (3.3), and thus we acquire the following expression in terms of variables $\varrho$

$$\overline{b}_q\varrho_{n-1}^q + \overline{c}_q\varrho_n^q + \overline{d}_q\varrho_{n+1}^q = \Phi_n^{q-1}, \quad 0 \leq n \leq N_z,\ 0 \leq q \leq M_t, \tag{5.2}$$

where

$$\Phi_n^{q-1}=\overline{k}_{q-1}\varrho_{n-1}^{q-1}+\overline{l}_{q-1}\varrho_n^{q-1}+\overline{m}_{q-1}\varrho_{n+1}^{q-1}-S\tau\sum_{j=0}^{q-1}B_j^qP_n^j-S\tau\sum_{j=0}^{q-2}D_j^{q-1}P_n^j+\tau g_n^{q-1/2},$$

$$\overline{b}_q=\left(SB_q^q+\frac{\hat{\beta}}{\tau}+\frac{\hat{\gamma}}{2}\right)\tau a_1-\frac{\hat{\nu}\tau}{2}a_4-\frac{\hat{\mu}\tau}{2}a_3,\quad \overline{c}_q=\left(SB_q^q+\frac{\hat{\beta}}{\tau}+\frac{\hat{\gamma}}{2}\right)\tau a_2-\frac{\hat{\nu}\tau}{2}a_5,$$

$$\overline{d}_q=\left(SB_q^q+\frac{\hat{\beta}}{\tau}+\frac{\hat{\gamma}}{2}\right)\tau a_1-\frac{\hat{\nu}\tau}{2}a_4+\frac{\hat{\mu}\tau}{2}a_3,$$

$$\overline{k}_{q-1}=\left(-SD_{q-1}^{q-1}+\frac{\hat{\beta}}{\tau}-\frac{\hat{\gamma}}{2}\right)\tau a_1+\frac{\hat{\nu}\tau}{2}a_4+\frac{\hat{\mu}\tau}{2}a_3],$$

$$\overline{l}_{q-1}=\left(-SD_{q-1}^{q-1}+\frac{\hat{\beta}}{\tau}-\frac{\hat{\gamma}}{2}\right)\tau a_2+\frac{\hat{\nu}\tau}{2}a_5],$$

$$\overline{m}_{q-1}=\left(-SD_{q-1}^{q-1}+\frac{\hat{\beta}}{\tau}-\frac{\hat{\gamma}}{2}\right)\tau a_1+\frac{\hat{\nu}\tau}{2}a_4-\frac{\hat{\mu}\tau}{2}a_3],$$

and

$$P_n^j=a_1\varrho_{n-1}^j+a_2\varrho_n^j+a_1\varrho_{n+1}^j,\quad j=0,1,\ldots,q.$$

The two additional equations obtained from boundary conditions that are used to solve the system (5.2) are given as

$$\varrho_{-1}^q=\frac{1}{a_1}(\phi_0^q-a_2\varrho_0^q)-\varrho_1^q\quad\text{and}\quad\varrho_{N_z+1}^q=\frac{1}{a_1}(\phi_1^q-a_2\varrho_{N_z}^q)-\varrho_{N_z-1}^q.\tag{5.3}$$

Thus, we have the tri-diagonal system in the form

$$B\varrho^q=J^{q-1},\tag{5.4}$$

where

$$B=\begin{bmatrix}\frac{\hat{\eta}\tau}{2}\left(\frac{a_2a_4}{a_1}-a_5\right)+\frac{\hat{\mu}\tau}{2}\frac{a_2a_3}{a_1} & \hat{\mu}\tau a_3 & 0 & \ldots\ldots & \ldots & 0\\ \overline{b}_q & \overline{c}_q & \overline{d}_q & & & \vdots\\ 0 & \ldots & \ldots\ldots & & & \vdots\\ \vdots & & & \overline{b}_q & \overline{c}_q & \overline{d}_q\\ 0 & \ldots & \ldots\ldots & 0 & -\hat{\mu}\tau a_3 & \frac{\hat{\eta}\tau}{2}\left(\frac{a_2a_4}{a_1}-a_5\right)-\frac{\hat{\mu}\tau}{2}\frac{a_2a_3}{a_1}\end{bmatrix},$$

$\varrho^q=(\varrho_0^q,\varrho_1^q,\ldots,\varrho_{N_z-1}^q,\varrho_{N_z}^q)^T$ and $J^{q-1}=\left(\Phi_0^{q-1}-\frac{\overline{b}_q\phi_0^q}{a_1},\Phi_1^{q-1},\ldots,\Phi_{N_z-1}^{q-1},\Phi_{N_z}^{q-1}-\frac{\overline{d}_q\phi_1^q}{a_1}\right)^T$.

**Lemma 5.1.** *The cubic trigonometric B-spline $TB_{-1},TB_0,\ldots,TB_{N_z+1}$ satisfy*

$$\sum_{n=-1}^{N_z+1}|TB_n(z)|\le 6,\ 0\le z\le 1.$$

**Proof.** Recall that $|\sum_{n=-1}^{N_z+1} TB_n(z)| \leq \sum_{n=-1}^{N_z+1} |TB_n(z)|$. For any point $z_j$, we can write the following statement

$$\sum_{n=-1}^{N_z+1} |TB_n(z_j)| = |TB_{n-1}(z_j)| + |TB_n(z_j)| + |TB_{n+1}(z_j)| = |a_1| + |a_2| + |a_1| \leq 4.$$

Consider any point in each subinterval $z_{j-1} < z < z_j$, then

$$\sum_{n=-1}^{N_z+1} |TB_n(z)| = |TB_{n-2}(z)| + |TB_{n-1}(z)| + |TB_n(z)| + |TB_{n+1}(z)| \leq 6.$$

Thus, for all $z \in [0,1]$, we have

$$\sum_{n=-1}^{N_z+1} |TB_n(z)| = |TB_{n-2}(z)| + |TB_{n-1}(z)| + |TB_n(z)| \leq 6.$$

Hence, the lemma is proved. □

**Lemma 5.2** ( [3, 13]). *Let the unique CTBS that interpolates the solution $u(z,t)$ of the problem (1.1) be $U(z,t)$. If $u(z,t) \in C^4[0,1]$, then there exist constants $\mathfrak{c}_k$, such that $\forall\ t \geq 0$*

$$\|D^k(u(z,t) - U(z,t))\|_\infty \leq \mathfrak{c}_k h^{4-k},\ k = 0, 1, 2.$$

**Theorem 5.1** ( [18]). *Let $U(z,t)$ be the CTBS approximation to the exact solution $u(z,t)$ of the problem (1.1). If $u(z,t) \in C^4[0,L]$ and $f \in C^2[0,L]$ then there exist a constant $K$, such that*

$$\|u(z,t) - U(z,t)\|_\infty \leq Kh^2.$$

**Proof.** Let $\widetilde{U}(z,t) = \sum_{n=-1}^{N_z+1} \varrho_n(t) TB_n(z)$ be the unique CTBS interpolation to the exact solution of the given problem (1.1) and $U(z,t) = \sum_{n=-1}^{N_z+1} \lambda_n(t) TB_n(z)$ be the approximate CTBS of equation (1.1). To prove the above result, we will evaluate the two terms $\|u(z,t) - \widetilde{U}(z,t)\|_\infty$ and $\|U(z,t) - \widetilde{U}(z,t)\|_\infty$. From equation (5.4), we have

$$B\varrho^q = J^{q-1}, \quad q = 1, 2, \ldots, M_t, \tag{5.5}$$

and

$$B\lambda^q = \widetilde{J}^{q-1}, \quad q = 1, 2, \ldots, M_t, \tag{5.6}$$

where $\lambda^q = (\lambda_0^q, \lambda_1^q, \ldots, \lambda_{N_z-1}^q, \lambda_{N_z}^q)$ and $\widetilde{J}^{q-1} = \left(\widetilde{\Phi}_0^{q-1} - \frac{\bar{b}_q \phi_0^q}{a_1}, \widetilde{\Phi}_1^{q-1}, \ldots, \widetilde{\Phi}_{N_z-1}^{q-1}, \widetilde{\Phi}_{N_z}^{q-1} - \frac{\bar{d}_q \phi_1^q}{a_1}\right)$.

Subtracting Equation (5.6) from (5.5), we get

$$B(\varrho^q - \lambda^q) = J^{q-1} - \widetilde{J}^{q-1},\ q = 1, 2, \ldots, M_t, \tag{5.7}$$

where $J^{q-1} - \widetilde{J}^{q-1} = (\Phi_0^{q-1} - \widetilde{\Phi}_0^{q-1}, \Phi_1^{q-1} - \widetilde{\Phi}_1^{q-1}, \ldots, \Phi_{N_z}^{q-1} - \widetilde{\Phi}_{N_z}^{q-1})$.

Now, consider the following condition

$$\begin{aligned}
&\left|\Phi_n^{q-1} - \widetilde{\Phi}_n^{q-1}\right| \\
&\leq \left|\hat{\beta} - S\tau D_{q-1}^{q-1} - \frac{\hat{\gamma}\tau}{2}\right| \left|U(z_n, t_{q-1}) - \widetilde{U}(z_n, t_{q-1})\right| + \frac{\hat{\nu}\tau}{2} \left|U_{zz}(z_n, t_{q-1}) - \widetilde{U}_{zz}(z_n, t_{q-1})\right|
\end{aligned}$$

$$+\frac{\hat{\mu}\tau}{2}\Big|U_z(z_n,t_{q-1})-\widetilde{U}_z(z_n,t_{q-1})\Big|+\Big|-S\tau\sum_{j=0}^{q-1}B_j^q\Big|\Big|U(z_n,t_j)-\widetilde{U}(z_n,t_j)\Big|$$

$$+\Big|-S\tau\sum_{j=0}^{q-2}D_j^{q-1}\Big|\Big|U(z_n,t_j)-\widetilde{U}(z_n,t_j)\Big|. \tag{5.8}$$

From Lemma 5.2 and Equation (5.8), we have

$$\begin{aligned}\|J^{q-1}-\widetilde{J}^{q-1}\|_\infty \leq& \Big|\hat{\beta}-S\tau D_{q-1}^{q-1}-\frac{\hat{\gamma}\tau}{2}\Big|\mathfrak{c}_0h^4+\frac{\hat{\nu}\tau}{2}\mathfrak{c}_2h^2+\frac{\hat{\mu}\tau}{2}\mathfrak{c}_1h^3\\ &+\mathfrak{c}_0h^4\left(\Big|-S\tau\sum_{j=0}^{q-1}B_j^q\Big|+\Big|-S\tau\sum_{j=0}^{q-2}D_j^{q-1}\Big|\right)\\ =&\mathfrak{M}h^2,\end{aligned} \tag{5.9}$$

where $\mathfrak{M}=\left(\Big|\hat{\beta}-S\tau D_{q-1}^{q-1}-\frac{\hat{\gamma}\tau}{2}\Big|+S\tau B_q^q+S\tau D_{q-1}^{q-1}\right)\mathfrak{c}_0h^2+\frac{\hat{\nu}\tau}{2}\mathfrak{c}_2+\frac{\hat{\mu}\tau}{2}\mathfrak{c}_1h.$

Since the matrix $B$ is strictly diagonally dominant for appropriately enough small $h$ and hence invertible, so from Equation (5.7), we obtain

$$\|\varrho^q-\lambda^q\|_\infty\leq\|B^{-1}\|_\infty\|J^{q-1}-\widetilde{J}^{q-1}\|_\infty. \tag{5.10}$$

The row sums $r_0,r_1,\ldots,r_{N_z}$ of the matrix $B$ are as follows

$$\begin{aligned}r_0&=\frac{\hat{\eta}\tau}{2}\Big(\frac{a_2a_4}{a_1}-a_5\Big)+\frac{\hat{\mu}\tau}{2}\Big(\frac{a_2a_3}{a_1}+2a_3\Big),\\ r_n&=\overline{b}_q+\overline{c}_q+\overline{d}_q,\ n=1,2,\ldots,N_z-1,\end{aligned}$$

and

$$r_{N_z}=\frac{\hat{\eta}\tau}{2}\Big(\frac{a_2a_4}{a_1}-a_5\Big)-\frac{\hat{\mu}\tau}{2}\Big(\frac{a_2a_3}{a_1}+2a_3\Big).$$

Using the theory of matrices, we obtain

$$\|B^{-1}\|_\infty\leq\frac{1}{r}\leq\frac{1}{|r|}, \tag{5.11}$$

where $r=\min\{r_0,r_1,\ldots,r_{N_z}\}$.

Now, by using the inequalities (5.9) and (5.11) into the inequality (5.10), we get

$$\|\varrho^q-\lambda^q\|_\infty\leq\frac{\mathfrak{M}h^2}{|r|}. \tag{5.12}$$

Now using Lemma 5.1 and the inequality (5.12), we obtain the following bound

$$\|U(z,t)-\widetilde{U}(z,t)\|_\infty=\left\|\sum_{n=-1}^{N_z+1}(\varrho_n-v\lambda_n)TB_n(z)\right\|_\infty\left|\sum_{n=-1}^{N_z+1}TB_n(z)\right|\|\varrho-\lambda\|_\infty\leq\frac{6\mathfrak{M}h^2}{|r|}. \tag{5.13}$$

On applying theorem 5.1, we get

$$\|u(z,t)-\widetilde{U}(z,t)\|_\infty\leq\mathfrak{c}_0h^4. \tag{5.14}$$

Thus, from Equations (5.13) and (5.14), we conclude that

$$\|u(z,t) - U(z,t)\|_\infty \leq Kh^2,$$

where $K = \mathfrak{c}_0 h^2 + \frac{6\mathfrak{M}}{|r|}$.

Hence, we proved the required condition stated in the theorem. □

**Theorem 5.2.** *The proposed numerical scheme (5.2) to solve the problem (1.1) is convergent of order of accuracy $O(\tau^2 + h^2)$.*

**Proof.** The numerical and exact solutions to the problem (1.1) be considered as $u(z,t)$ and $U(z,t)$, respectively. By applying Theorem 5.1 and using the relation defined in Equation (2.4), we obtain

$$\|u(z,t) - U(z,t)\|_\infty \leq \mathfrak{C}(\tau^2 + h^2),$$

where $\mathfrak{C}$ is a constant.

Therefore, the numerical scheme (5.2) converges to the second order. □

# 6. Numerical Illustrations

This section illustrates two test examples that authenticate the computational algorithm and theoretical findings. However, the convergence of the numerical scheme presented in (3.6) is shown in the $l^2$-norm. For the demonstration purpose, the error is computed in the $l^2$, and the maximum norm is defined as follows

$$E_2^{N_z,M_t} = \|U - u\|_2 = \max_{0\leq q\leq M_t} \sqrt{h\sum_{n=0}^{N_z} |U(z_n,t_q) - u_n^q)|^2},$$
$$E_\infty^{N_z,M_t} = \|U - u\|_\infty = \max_{0\leq q\leq M_t} (\max_{0\leq n\leq N_z} |U(z_n,t_q) - u_n^q)|).$$

In addition, to demonstrate the numerical scheme's high precision, we compute its order of convergence $\mathrm{ord}_p^{N_z,M_t}$ as

$$\mathrm{ord}_p^{N_z,M_t} = \frac{\ln(\mathrm{E}_p^{N_z,M_t}/\mathrm{E}_p^{2N_z,2M_t})}{\ln 2}, \quad p = 2,\infty.$$

To demonstrate the effectiveness of the proposed numerical scheme, various results are presented in the form of tables and graphs. All the graphs are displayed using $N_z = M_t = 64$, and the tabulated results are obtained using $N_z = M_t$. The domain $\Omega_z \in [0,1]$ with $T = 1$ is considered for both examples representing the problem (1.1). The results presented in Tables 1 and 2 validate the efficacy and precision of the new scheme. The proposed numerical technique is accurate to the second order, as evidenced by the convergence orders in these tables.

Figure 1(a) presents the numerical solution behavior at $\alpha = 0.5$. This 3D plot shows that as we increase the grid points in the space and time direction, the numerical solution increases initially, reaches a maximum, and decreases gradually. Figure 1(b) depicts the obtained solution behavior at various time levels. For this one-dimensional plot, we have to fix the number of grid points in the space direction so that the variations of numerical solutions at distinct time levels are observed. The

solution obtained using our numerical technique is quite close to the exact solution, as shown by line plots of the numerical and exact solutions in Figure 2. Figure 3 illustrates the behavior of the error in the $l^2$-norm that occurs while computing the numerical solution.

**Example 6.1.** Consider the problem (1.1) with $\beta = 3zt$, $\nu = \cos(zt)$, $\mu = z^2$, and $\gamma = z + 2$. In addition, the exact solution of the equation $u = (z^3 - 2z^2 + z)t^4$ is used to compute the conditions (1.1b), (1.1c) and (1.1d) as well as the source term $g(z, t)$.

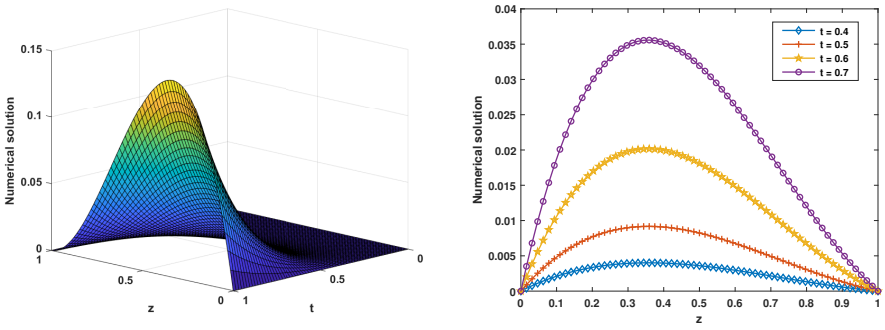


(a) (b)

**Figure 1.** Plots depicting the behavior of numerical solution at $\alpha = 0.5$ for Example 6.1

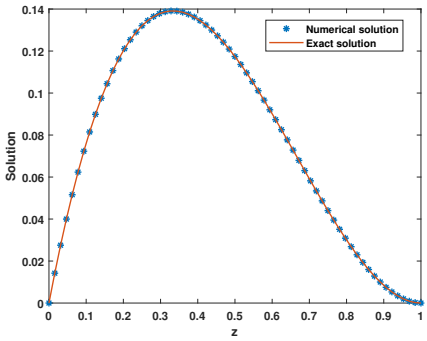


**Figure 2.** Line plots of the exact and numerical solutions for Example 6.1 at $t = 0.5$ for $\alpha = 0.5$

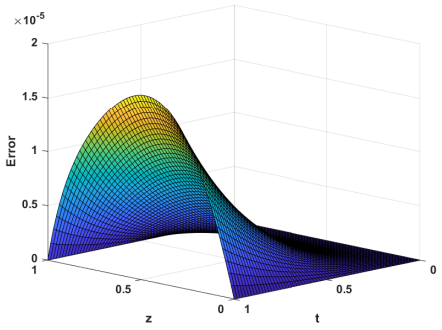


**Figure 3.** Error plot for $\alpha = 0.5$ for Example 6.1

**Example 6.2.** Consider the problem (1.1) with $\beta = \sin(zt)$, $\nu = z + 1$, $\mu = z$, and $\gamma = zt$. In addition, the exact solution of the equation $u = -\sin(\pi z)t^4$ is used to compute the conditions (1.1b), (1.1c) and (1.1d) as well as the source term $g(z, t)$.

To strengthen the arguments given above, we consider another example (Application 6.2). We have also provided the numerical findings in tables and graphs to support the theoretical results. The solution to the problem in Example 6.2 is displayed in Figure 4. Moreover, Figure 5 illustrates that the numerical solution

**Table 1.** $l^2$-norm errors and orders of convergence for Example 6.1

| | No. of grid points | | | | |
|---|---|---|---|---|---|
| $\alpha$ | 16 | 32 | 64 | 128 | 256 |
| 0.1 | $7.8434e-04$ | $1.9383e-04$ | $4.8343e-05$ | $1.2083e-05$ | $3.0217e-06$ |
| | 2.0167 | 2.0034 | 2.0003 | 1.9995 | |
| 0.3 | $7.9642e-04$ | $1.9737e-04$ | $4.9326e-05$ | $1.2348e-05$ | $3.0916e-06$ |
| | 2.0126 | 2.0005 | 1.9981 | 1.9979 | |
| 0.5 | $8.2186e-04$ | $2.0438e-04$ | $5.1167e-05$ | $1.2819e-05$ | $3.2106e-06$ |
| | 2.0076 | 1.9980 | 1.9969 | 1.9974 | |
| 0.7 | $8.9392e-04$ | $2.2351e-04$ | $5.6052e-05$ | $1.4048e-05$ | $3.5178e-06$ |
| | 1.9998 | 1.9955 | 1.9964 | 1.9976 | |
| 0.9 | $1.3550e-03$ | $3.4809e-04$ | $8.7990e-05$ | $2.2097e-05$ | $5.5350e-06$ |
| | 1.9608 | 1.9840 | 1.9935 | 1.9972 | |

**Table 2.** Maximum norm errors and orders of convergence for Example 6.1

| | No. of grid points | | | | |
|---|---|---|---|---|---|
| $\alpha$ | 16 | 32 | 64 | 128 | 256 |
| 0.1 | $1.0365e-03$ | $2.5691e-04$ | $6.4144e-05$ | $1.6048e-05$ | $4.0135e-0$ |
| | 2.0124 | 2.0019 | 1.9989 | 1.9995 | |
| 0.3 | $1.0536e-03$ | $2.6191e-04$ | $6.5571e-05$ | $1.6427e-05$ | $4.1138e-06$ |
| | 2.0082 | 1.9979 | 1.9970 | 1.9975 | |
| 0.5 | $1.0897e-03$ | $2.7181e-04$ | $6.8248e-05$ | $1.7106e-05$ | $4.2856e-06$ |
| | 2.0033 | 1.9937 | 1.9963 | 1.9969 | |
| 0.7 | $1.1912e-03$ | $2.9896e-04$ | $7.5311e-05$ | $1.8882e-05$ | $4.7291e-06$ |
| | 1.9944 | 1.9890 | 1.9958 | 1.9974 | |
| 0.9 | $1.8358e-03$ | $4.7943e-04$ | $1.2134e-04$ | $3.0482e-05$ | $7.6363e-06$ |
| | 1.9370 | 1.9823 | 1.9930 | 1.9970 | |

agrees with the exact solution. Meanwhile, in Figure 6, we plot the errors in the $l^2$-norm for different values of $z$ and $t$ with $\alpha = 0.9$. The results show the overall accuracy, which aligns well with the theoretical analysis. In addition, Tables 3 and 4 show the errors and the orders of convergence in the $l^2$ and the maximum norms, respectively, for various values of $\alpha$. These tabular results reveal that the convergence order is two in both norms.

# 7. Conclusions

This article focuses on the numerical analysis of the time-fractional mobile-immobile solute transport equation with variable coefficients using a numerical technique comprising CTBS in the spatial direction and the Crank-Nicolson scheme in the tem-

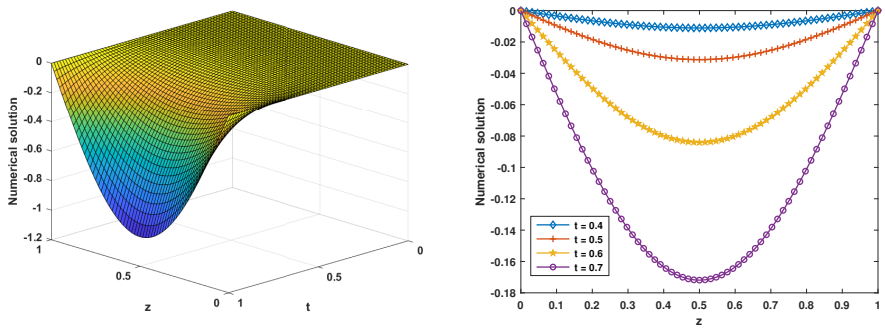


(a) (b)

**Figure 4.** Plots depicting the behavior of numerical solution at $\alpha = 0.9$ for Example 6.2

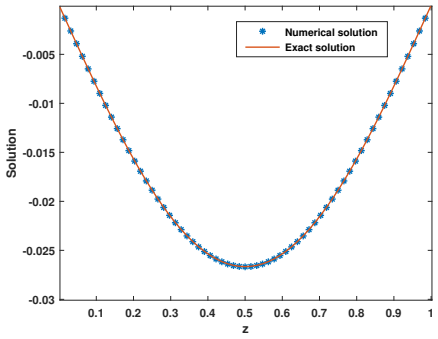


**Figure 5.** Line plots of the exact and numerical solution for Example 6.2 for $\alpha = 0.9$ at $t = 0.5$

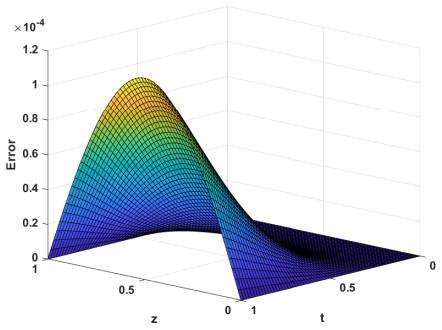


**Figure 6.** Error plot for $\alpha = 0.9$ for Example 6.2

**Table 3.** $l^2$-norm errors and orders of convergence for Example 6.2

| | No. of grid points | | | | |
|---|---|---|---|---|---|
| $\alpha$ | 16 | 32 | 64 | 128 | 256 |
| 0.1 | $6.1130e-04$ | $1.5179e-04$ | $3.7831e-05$ | $9.4386e-06$ | $2.3556e-06$ |
| | 2.0098 | 2.0044 | 2.0029 | 2.0025 | |
| 0.3 | $5.5883e-04$ | $1.3753e-04$ | $3.4048e-05$ | $8.4507e-06$ | $2.1006e-07$ |
| | 2.0227 | 2.0141 | 2.0104 | 2.0083 | |
| 0.5 | $4.5358e-04$ | $1.1018e-04$ | $2.7083e-05$ | $6.6960e-06$ | $1.6613e-06$ |
| | 2.0415 | 2.0244 | 2.0160 | 2.0110 | |
| 0.7 | $1.9569e-04$ | $4.4480e-05$ | $1.0571e-05$ | $2.5687e-06$ | $6.3984e-07$ |
| | 2.1373 | 2.0730 | 2.0410 | 2.0053 | |
| 0.9 | $1.0417e-03$ | $2.5458e-04$ | $6.2465e-05$ | $1.5450e-05$ | $3.7024e-06$ |
| | 2.0327 | 2.0270 | 2.0154 | 2.0611 | |

**Table 4.** Maximum norm errors and orders of convergence for Example 6.2

| | No. of grid points | | | | |
|---|---|---|---|---|---|
| $\alpha$ | 16 | 32 | 64 | 128 | 256 |
| 0.1 | $3.4789e-03$ | $8.5591e-04$ | $2.1282e-04$ | $5.3070e-05$ | $1.3241e-05$ |
| | 2.0231 | 2.0078 | 2.0037 | 2.0029 | |
| 0.3 | $3.2182e-03$ | $7.8281e-04$ | $1.9277e-04$ | $4.7768e-05$ | $1.1856e-05$ |
| | 2.0395 | 2.0218 | 2.0128 | 2.0104 | |
| 0.5 | $2.6698e-03$ | $6.3614e-04$ | $1.5457e-04$ | $3.8001e-05$ | $9.3982e-06$ |
| | 2.0693 | 2.0411 | 2.0242 | 2.0156 | |
| 0.7 | $1.3170e-03$ | $2.7679e-04$ | $6.3363e-05$ | $1.5115e-05$ | $3.6786e-06$ |
| | 2.2504 | 2.1271 | 2.0677 | 2.0388 | |
| 0.9 | $6.1364e-03$ | $1.7533e-03$ | $4.5824e-04$ | $1.1642e-04$ | $2.9294e-05$ |
| | 1.8073 | 1.9359 | 1.9768 | 1.9907 | |

poral direction. The time derivative of fractional order is numerically investigated using the definition given by Atangana and Baleanu in Caputo sense, and a new numerical formulation is presented for fractional time derivative. The proposed numerical approach involves the average of time fractional derivative at $q^{th}$ and $(q-1)^{th}$ level that will increase the time convergence order and give better results than the numerical schemes presented in the existing literature for this problem. We have shown that our scheme is unconditionally stable through the Von-Neumann stability analysis method. Theoretically, the proposed scheme is proved to be accurate of order $O(\tau^2 + h^2)$ in the maximum norm. Also, from Tables 2 and 4, it can be observed that the method is second-order accurate in the maximum norm. Moreover, from the line and surface plots, we have demonstrated that the solution obtained by applying our numerical technique matches the exact one. In future studies, we will use the suggested approach to other time-fractional applications in various fields.

**Declaration of Competing Interest.** The authors state that they have no known competing financial interests or personal ties that could have influenced the research presented in this study.

**Data Availability Statement.** Data sharing does not apply to this article as no datasets were generated or analyzed during the current study.

**Acknowledgement.** The authors would like to express their heartfelt gratitude to the anonymous reviewers for their many insightful remarks and corrections.

# References

[1] A. Atangana and D. Baleanu, *New fractional derivatives with non-local and non-singular kernel: theory and application to heat transfer model*, Therm. Sci., 2016, 20, 763–769.

[2] E. Bas and R. Ozarslan, *Real world applications of fractional models by*

*Atangana-Baleanu fractional derivative*, Chaos Solitions Fractals, 2018, 116, 121–125.

[3] C. D. Boor, *On the convergence of odd-degree spline interpolation*, J. Approx. Theory, 1968, 1(4), 452–463.

[4] M. Caputo and M. Fabrizio, *A new definition of fractional derivative without singular kernel*, Progr. Fract. Differ. Appl., 2015, 1(2), 73–85.

[5] R. Chawla, K. Deswal, D. Kumar and D. Baleanu, *A novel finite difference based numerical approach for Modified Atangana-Baleanu Caputo derivative*, AIMS Math., 2022, 7(9), 17252–17268.

[6] R. Chawla, K. Deswal and D. Kumar, *A new numerical formulation for the generalized time-fractional Benjamin Bona Mohany Burgers' equation*, Int. J. Nonlinear Sci. Numer. Simul., 2022. DOI: 10.1515/ijnsns-2022-0209.

[7] C. Chen, H. Liu, X. Zheng and H. Wang, *A two-grid MMOC finite element method for nonlinear variable-order time-fractional mobile/immobile advection-diffusion equations*, Comput. Math. Appl., 2020, 79(9), 2771–2783.

[8] G. Gao, H. Zhan, S. Feng, B. Fu, Y. Ma and G. Huang, *A new mobile-immobile model for reactive solute transport with scale-dependent dispersion*, Water Resour. Res., 2010. DOI: 10.1029/2009WR008707.

[9] G. Gao and Z. Sun, *A compact finite difference scheme for the fractional sub-diffusion equations*, J. Comput. Phys., 2011, 230(3), 586–595.

[10] W. Gao, B. Ghanbari and H. M. Baskonus, *New numerical simulations for some real world problems with Atangana-Baleanu fractional derivative*, Chaos Solitions Fractals, 2019, 128, 34–43.

[11] H. R. Ghehsareh, A. Zaghian and M. Raei, *A local weak form meshless method to simulate a variable order time-fractional mobile-immobile transport model*, Eng. Anal. Bound. Elem., 2018, 90, 63–75.

[12] A. Golbabai, O. Nikan and T. Nikazad, *Numerical investigation of the time fractional mobile-immobile advection-dispersion model arising from solute transport in porous media*, Int. J. Appl. Comput. Math., 2019, 5, 1–22.

[13] C. A. Hall, *On error bounds for spline interpolation*, J. Approx. Theory, 1968, 1(2), 209–218.

[14] M. Hamid, M. Usman, R. U. Haq and W. Wang, *A Chelyshkov polynomial based algorithm to analyze the transport dynamics and anomalous diffusion in fractional model*, Physica A, 2020, 551, 124227.

[15] A. A. Hamou, E. H. Azroul, Z. Hammouch and A. L. Alaoui, *A monotone iterative technique combined to finite element method for solving reaction-diffusion problems pertaining to non-integer derivative*, Eng. Comput., 2022, DOI: 10.1007/s00366-022-01635-4.

[16] M. H. Heydari and A. Atangana, *An optimization method based on the generalized Lucas polynomials for variable-order space-time fractional mobile-immobile advection-dispersion equation involving derivatives with non-singular kernels*, Chaos Solitions Fractals, 2020, 132, 109588.

[17] A. S. V. Kanth and S. Deepika, *Application and analysis of spline approximation for time fractional mobile-immobile advection-dispersion equation*, Numer. Methods Partial Differ. Equ., 2018, 34(5), 1799–1819.

[18] A. S. V. Kanth and N. Garg, *A numerical approach for a class of time-fractional reaction-diffusion equation through exponential B-spline method*, Comput. Appl. Math., 2020, 39, 1–24.

[19] A. Kumar, A. Bhardwaj and B. V. R. Kumar, *A meshless local collocation method for time fractional diffusion wave equation*, Comput. Math. Appl., 2019, 78(6), 1851–1861.

[20] A. A. Kilbas, H. M. Srivastava and J. J. Trujillo, *Theory and Applications of Fractional Differential Equations*, Elsevier Science, Publishers BV, Amsterdam, 2006.

[21] X. Li, Z. Wen, Q. Zhu and H. Jakada, *A mobile-immobile model for reactive solute transport in a radial two-zone confined aquifer*, J. Hydrol., 2020, 580, 124347.

[22] F. Liu, P. Zhuang, I. Turner, K. Burrage and V. Anh, *A new fractional finite volume method for solving the fractional diffusion equation*, Appl. Math. Model., 2014, 38(15–16), 3871–3878.

[23] Y. Liu, M. Zhang, H. Li and J. Li, *High-order local discontinuous Galerkin method combined with WSGD-approximation for a fractional subdiffusion equation*, Comput. Math. Appl., 2017, 73(6), 1298–1314.

[24] Z. Liu and X. Li, *A Crank-Nicolson difference scheme for the time variable fractional mobile-immobile advection-dispersion equation*, J. Appl. Math. Comput., 2018, 56(1–2), 391–410.

[25] Z. Liu, X. Li and X. Zhang, *A fast high-order compact difference method for the fractal mobile/immobile transport equation*, Int. J. Appl. Comput. Math., 2020, 97(9), 1860–1883.

[26] B. Maayah, O. A. Arqub, S. Alnabulsi and H. Alsulami, *Numerical solutions and geometric attractors of a fractional model of the cancer-immune based on the Atangana-Baleanu-Caputo derivative and the reproducing kernel scheme*, Chinese J. Phys., 2022, 80, 463–483.

[27] P. Perdikaris and G. E. Karniadakis, *Fractional-order viscoelasticity in one-dimensional blood flow models*, Ann. Biomed. Eng., 2014, 42, 1012–1023.

[28] I. Podlubny, *Fractional Differential Equations*, Academic Press, San Diego, 1999.

[29] S. S. Ray, *A novel wavelets operational matrix method for the time variable-order fractional mobile-immobile advection-dispersion model*, Eng. Comput., 2021. DOI: 10.1007/s00366-021-01405-8.

[30] K. Sadri and H. Aminikhah, *An efficient numerical method for solving a class of variable-order fractional mobile-immobile advection-dispersion equations and its convergence analysis*, Chaos Solitions Fractals, 2021, 146, 110896.

[31] R. Schumer, D. A. Benson, M. M. Meerschaert and B. Baeumer, *Fractal mobile/immobile solute transport*, Water Resour. Res., 2003, 39(10), 1296.

[32] M. Saffarian and A. Mohebbi, *An efficient numerical method for the solution of 2D variable order time fractional mobile-immobile advection-dispersion model*, Math. Meth. Appl. Sci., 2021, 44(7), 5908–5929.

[33] M. Shafiq, M. Abbas, K. M. Abualnaja, A. Majeed and T. Nazir, *An efficient technique based on cubic B-spline functions for solving time-fractional advection diffusion equation involving Atangana-Baleanu derivative*, Eng. Comput., 2021. DOI: 10.1007/s00366-021-01490-9.

[34] F. Song and C. Xu, *Spectral direction splitting methods for two-dimensional space fractional diffusion equations*, J. Comput. Phys., 2015, 299, 196–214.

[35] X. Yang, H. Zhang and Q. tang, *A spline collocation method for a fractional mobile-immobile equation with variable coefficients*, Comput. Appl. Math., 2020. DOI:10.1007/s40314-019-1013-3.

[36] M. Zhang, Y. Liu and H. Li, *High-order local discontinuous Galerkin method for a fractal mobile/immobile transport equation with the Caputo-Fabrizio fractional derivative*, Numer. Methods Partial Differ. Equ., 2019, 35(4), 1588–1612.

[37] Y. Zhao, W. Bu, J. Huang, D. Liu and Y. Tang, *Finite element method for two-dimensional space-fractional advection-dispersion equations*, Appl. Math. Comput., 2015, 257, 553–565.